ISSN: 1687-1006 p
ISSN: 2682-3640 e

The Egyptian International Journal of Engineering Sciences and Technology

Vol. 32 (2020) 73–79

https://eijest.journals.ekb.eg/

Performance Enhancement of the Fluidyne Pump

Mahdy Megahed*, Hafez Elsalmawy, Mohamed A. Essa

Department of Mechanical Power Engineering, Faculty of Engineering, Zagazig University, 44519 Zagazig, Egypt.

ARTICLE INFO

Keywords:

Fluidyne,
Liquid piston
Stirling engine,
Renewable liquid pumping.

ABSTRACT

In this work, an analysis of the governing equations of the fluidyne pump has been carried out to identify the design and operating parameters, which affect the performance of the fluidyne pump, such that the pump performance can be enhanced through the optimum tune up of these parameters. The impact of these parameters has been evaluated through two performance indicators including the non-dimensional pump flow rate and efficiency. The results showed that the three main controlling parameters are; gas to liquid volume ratio, the input energy intensity and the pumping pressure to displacer length ratio. It has been found that as working gas to working liquid volume ratio is higher, the efficiency of the fluidyne pump improves. Yet this is limited by the difference (2 PoTi /ρw*g*Ld) -(Vg / Vw), which should not be negative, also maximum flow rate and efficiency can be achieved as the difference becomes minimum. Also, both efficiency and non-dimensional flow rate improve as the heat added per unit of the working gas volume is higher. Furthermore, it improves the pump startup time due to the onset time for oscillation becomes less. These results are verified experimentally using an experimental model of the fluidyne pump, which is equipped with the necessary measuring instruments, where the test parameters can be changed independently to evaluate their impact. Good convergence between the computational results and the experimental measurements has been found.

1. Introduction

The fluidyne pump is a positive displacement liquid piston pump, which is driven by fluidyne engine. Fluidyne engine is classified as a type of Stirling engine (i.e. Alpha configuration) with liquid pistons [1]. Therefore, it can be driven by an external heat source. This heat source can be renewable such as solar energy. As being a type of renewable energy driven pump, the pump can be used for a wide range of applications as well as different types of liquids. Although the fluidyne pump has limitations regarding the flow rate and head [2], yet it has promising applications in several agricultural and industrial cases [3]. Fluidyne engine was originally developed in the U.K. at the Atomic energy Lab – 1971 by *C. West* [1]. It works according to "*Stirling cycle*" [2]. The cycle composes of two constant volume strokes and two constant temperature strokes, as illustrated in Fig.1. The pressure difference between the hot, the cold sides create a reciprocating movement for the working liquid generating output work. This reciprocating movement drives the pumping liquid column, which acts as positive displacement pump.

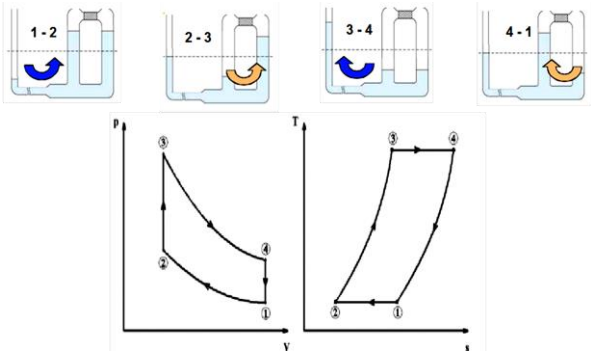

Fig.1 P-V and T-S diagram of fluidyne engine [2]

Several design features have been considered for the fluidyne engine. These include three main designs; Rocking beam, Pressure feedback and Jet stream feedback [2]. Considering the jet stream F.P. design, it includes several variations [3]. They are classified according to the position of the output tube, as shown in Fig-2.

* Corresponding author. Tel.: +2-01003934695
E-mail address: mahdynm@zu.edu.eg ;*mahdy_megahed@hotmail.com.*

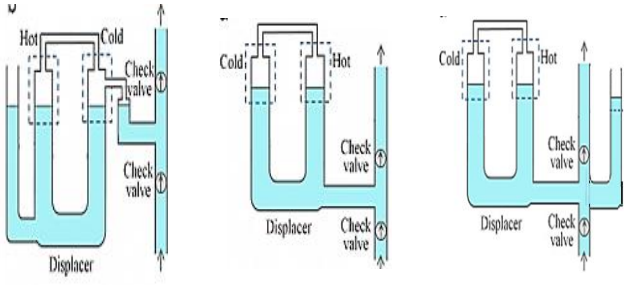

a- cold tube model b-series model c- Parallel model

Fig 2 –the main deigns for Jet Stream F.P. [4]

Several researchers have worked to improve the output and the frequency of operation of the engine and consequently the output power and efficiency. *West* [3] studied how to get a maximum output power through investigating the frequency and the amplitude of the system. *Elord* [4] studied the movement of cold, hot and output columns. *Goldberg* [5] investigated the threshold of the temperature difference needed to start the oscillations and consequently the pumping effect. *Mosby et al.* [1] tested the pump flow rate, stroke of the liquid piston and the onset temperature for the design of the fluidyne pump, shown in Fig.3. He considered three different gas volumes, and a temperature range (45-85 ^{0}C). They found that increasing gas volume and temperature of hot column increases in the displacement of the liquid piston and accordingly the output flow rate.

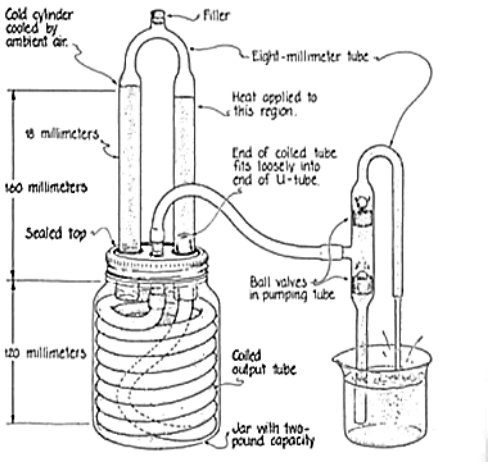

Fig.3 Mosby's model of the fuidyne Pump[1]

the biggest and more complicated model of F.P built by Harwell and Metal Box company [10], where the pump has a capacity of 1700 liter/hour, at 5-m head. The schematic drawing of this pump is shown in Fig. 4

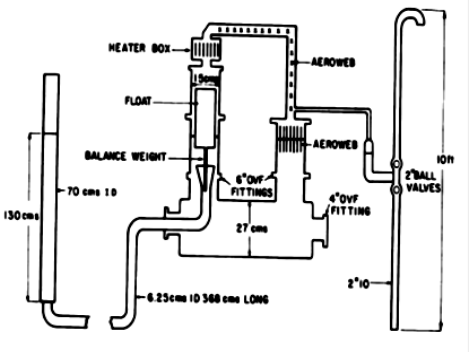

Fig 4 - Harwell and Metal Box company, pump [4]

Yamaguchi [9] showed that the output frequency depends on the output tube length, while the operational frequency depends on the working liquid height.

Table-1 shows that substantial enhancement has been achieved for the basic design over the following ten years, since the invent of the fluidyne pump. These enhancements have led to improvements in both the pump capacity and efficiency.

Table- 1 Development of models of fluidyne pump from 1970 to 1981

System		Q- litter/hour	Head (h) – m	η %
West (1971)	[3]	380	1.8	0.35
Goldberg et al. (1977)	[5]	36	0.7	0.12
Goldberg et al. (1977)	[5]	44	1	0.08
Mosby (1978)	[1]	22	0.4	0.15
Reader (1979)	[6]	.....	.....	0.03
Bell (1979)	[7]	114	1.2	0.18
Reader et al. (1981)	[6]	8	1.1	0.52
West et Pandey (1981)	[8]	1740	3.3	4.7
Pandey (1981)	[8]	9500	3.3	7

Due to its low efficiency, flow rate and limited head, compared with the mechanical pumping, interest in fluidyne pump became less during nineties and the first decay of the 21st century. Yet fluidyne pump has recently regained interest due to the development in the solar thermal systems and its simplicity [17]. *Jackson W. Mason et al.* [16] tested a free-unloaded fluidyne engine using a bank of Fresnel lens. They found that a ratio of 12% exists between the negative and positive work per cycle. *Frank Kyei and Obodoako 2006* [10] designed a FP, as shown in Fig.5. The pump has 4-Hz frequency and 25 cm amplitude. It has an output of 5 watts and its efficiency reached 3.5%.

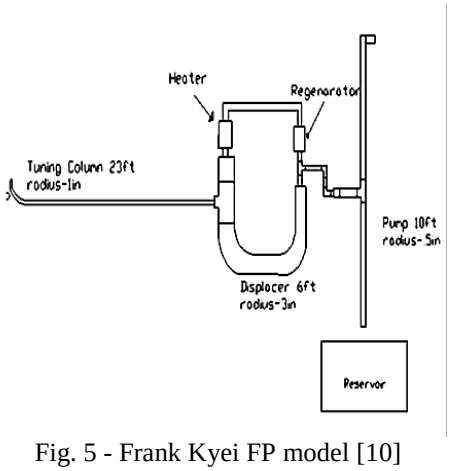

Fig. 5 - Frank Kyei FP model [10]

The objective of this work is to identify the controlling parameters, which have impact on the performance of the fluidyne pump, such that it become possible to optimize the operation of this pump through better tune up of these parameters. The governing equations of the fluidyne pump have been analyzed and compiled to identify the impact of the controlling parameters. An analysis is carried out to identify the best values of these parameters to achieve the highest possible performance indicators including efficiency and output flow rate. These results are verified experimentally using an experimental model of the fluidyne pump, which is equipped with necessary measuring instruments, where the test parameters can be changed independently to evaluate their impact.

2. Mathematical Formulation

The governing equations of the fluidyne engine can be expressed for two cases, loaded and un-loaded conditions. C. Stammers [2] solved the continuity, momentum and energy equations for the cold, hot, and output columns. For the solution. Several assumptions have been considered. These include; diameter of displacer tube is the same for the gas and the output tubes diameters. Initially the pressure in the gas tube is the same in both the hot and the cold zones. Regarding the cold zone temperatures in the gas tube, T_1 is almost fixed at 25°C, where the discharged water is used to keep this temperature fixed. For the hot zone $45^{o}c \leq T_2 \leq 90^{o}c$, such that liquid evaporation is avoided. Moreover, the output tube pressure is atmospheric. The properties of the working liquid inside the fluidyne engine and the pumped liquid are differentiated in the equation as: ρ_w and μ_w for working liquid, and ρ_o for pumped liquid. Based on the cycle analysis and according to the dimensions shown in Fig. 6, the governing equations of the fluidyne pump can be expressed as follows [1,2]:

$$\frac{T_2-T_1}{T_2+T_1} = \frac{\rho_w * V_g}{P_o * A_d}\left[\frac{0.5*g*L_d}{2H+L_d} + \frac{8\pi\mu_w}{(A_o*\rho_w)^2}\left(\frac{2H+L_d}{L_d}\right) b\right] \quad (1)$$

Also, the Fluidyne engine operation frequency for unloading condition, where ω can be expressed as follows [1]:

$$\omega_{un} = \sqrt{\frac{2g}{2H+L_d}} \quad (2)$$

On the other hand, the Fluidyne Pump (FP) operation frequency for loading condition ω_l . This can be correlated with total length of the output tube as follows [1]:

$$\omega_l = \sqrt{\frac{L_o \rho_w V_g}{P_o A_o}} \quad (3)$$

According to [2], theoretically load does not appreciably influence the frequency of operation. Therefore $\omega_{un} = \omega_l$.

For simplicity the working liquid length factor di and the temperature factor Ti can be expressed as:

$$d_i = \frac{L_d}{2H+L_d} \quad and \quad T_i = \frac{T_2-T_1}{T_2+T_1} .$$

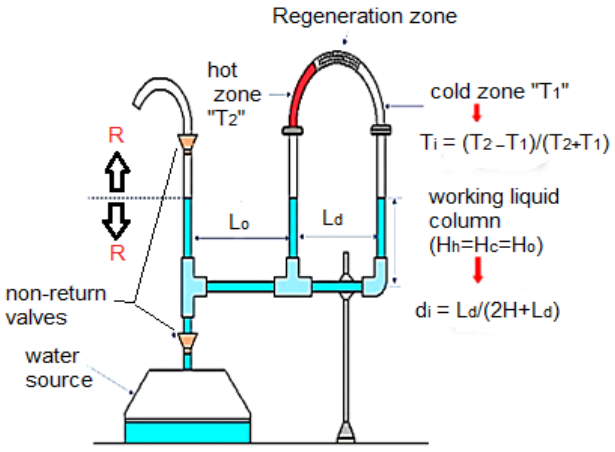

Figure-6 F.P. parameters

Considering the pump load, which has the following expression $\boldsymbol{Pump\ Load = \rho_o\, Q^o\, g\, h}$. By introducing the load coefficient b, which can take the following from [2]:

$$Pump\ Load = 0.5b(\omega_p R)^2$$
$$b = Load/\ (0.5\ (\omega_p R)^2$$

Since

$Q^o = 2RA_o/period\ time = \omega_p RA_o/\pi$

$\omega_p R = \pi\, \boldsymbol{Q^o}/A_o \qquad (\omega_p R)^2 = (\pi \boldsymbol{Q^o}/A_o)^2$

Accordingly, b can take the following form;

$$b = \rho_o\, g\, h\, /\, 0.5\boldsymbol{Q^o}\ (\pi/A_o)^2 \quad (4)$$

2.1 Flow Rate

Considering Eq. 4 and by Substituting in eq.(1) :

$$\frac{T_2-T_1}{T_2+T_1} = \frac{\rho_w * V_g}{P_o * A_d}\left[\frac{0.5*g*L_d}{2H+L_d} + \frac{8\pi\mu_w}{(A_o*\rho_w)^2}\left(\frac{2H+L_d}{L_d}\right) * \left(\frac{\rho_o\, \boldsymbol{Q^o} gh}{0.5\left(\frac{\pi \boldsymbol{Q^o}}{A_o}\right)^2}\right)\right] \quad (5)$$

Then:

$$\frac{T_2-T_1}{T_2+T_1} * \left(\frac{P_o * A_d}{V_g}\right) = 0.5\rho_w * g\left(\frac{L_d}{2H+L_d}\right) + \frac{8\mu_w}{\rho_w}\left(\frac{2H+L_d}{L_d}\right) * \left(\frac{\rho_o g h}{0.5\,\pi \boldsymbol{Q^o}}\right) \quad (6)$$

By rearranging, the pump flow rate can take the following expression:

$$\boldsymbol{Q^o} = \frac{\left(\frac{32}{d_i * d_i \pi}\right)\left(\frac{\mu_w}{\rho_w}\right) * h * \left(\frac{\rho_o}{\rho_w}\right)}{\left[\left[2\left(\frac{P_o}{\rho_w * g}\right) * \left(\frac{A_d}{V_g}\right) * \left(\frac{T_i}{d_i}\right)\right] - 1\right]} \quad (7)$$

Manipulating Eq. 7, Q^o can take the following form:

$$\boldsymbol{Q^o} = \frac{(\boldsymbol{10.19/d_i^2}) * \boldsymbol{\gamma_w} * \left(\frac{V_g}{V_w}\right) * \left(\frac{\rho_o}{\rho_w}\right)}{\boldsymbol{2\,Ti}\left(\frac{P_o}{\rho_w * g * L_d}\right) - \left(\frac{V_g}{V_w}\right)} * \boldsymbol{h} \quad (8)$$

It can be the general formula for different shapes of gas and liquid tubes

2.2 Output length (L_o)

According to Eq (3)

$$\boldsymbol{L_o = (P_o * A_o) / (\rho_w * V_g * \omega_p^2)} \quad \textbf{(9)}$$

Since, $\omega^2 = 2g/L_w$

$$L_o = 0.05\ (P_o/\rho_w)\ (L_w/L_g)(D_o/D_g)^2 \quad (10)$$

Table (2) output length approximate formula for different working liquids

Working liquid	water	Mercury	Olive oil
Output length	$5\left(\frac{Do}{Dg}\right)^2\left(\frac{Lw}{Lg}\right)$	$0.38\left(\frac{Do}{Dg}\right)^2\left(\frac{Lw}{Lg}\right)$	$5.45\left(\frac{Do}{Dg}\right)^2\left(\frac{Lw}{Lg}\right)$

For P_o=1 atm.

2.3 Efficiency

Since Efficiency: $\eta\% = \frac{\text{output work}}{\text{input power}} * 100$, Q_{in} is the input heat power and the pump demand equals $\rho_o\, Q^o\, g\, h$.

The pump efficiency can be expressed as follows:

$$\therefore\ \eta = \frac{(\rho_o * g * \gamma_w) * \left(\frac{10.19}{d_i^2}\right) * \left(\frac{V_g}{V_w}\right) * \left(\frac{\rho_o}{\rho_w}\right) * h^2}{Q_{in}\left[\left[2\,Ti\left(\frac{P_o}{L_d * g * \rho_w}\right)\right] - \left(\frac{V_g}{V_w}\right)\right]} \qquad (11)$$

2.4 Mathematical study results

Equation (11) shows that the independent nondimensional operational and design parameters, which affect the output indicators including flow rate and efficiency are: (T_i), (V_g / V_w), and ($\frac{P_o}{\rho_w * g * L_d}$). It elaborates that the difference of, $\left[\left[2\,Ti\left(\frac{P_o}{\rho_w * g * L_d}\right)\right] - \left(\frac{V_g}{V_w}\right)\right]$, is the main relation that affects the flow rate, and consequently the efficiency. Accordingly, as this difference is minimum, the flow rate, and as well as the efficiency will be higher. On the other hand this difference should be larger than zero, to avoid negative work (pumping water into the pump). Also, Q_{in} to the engine is an important parameter, which defines the Fluidyne pump efficiency. It is understood that T_i depends on Q_{in}/V_g. Where T_2 depends on Q_{in} while T_1 depends on the cold sink, which is normally cooled by the discharged water, which is almost fixed at 25°C (298 °K). Fig-7 shows the independent variables that control fluidyne pump flow rate.

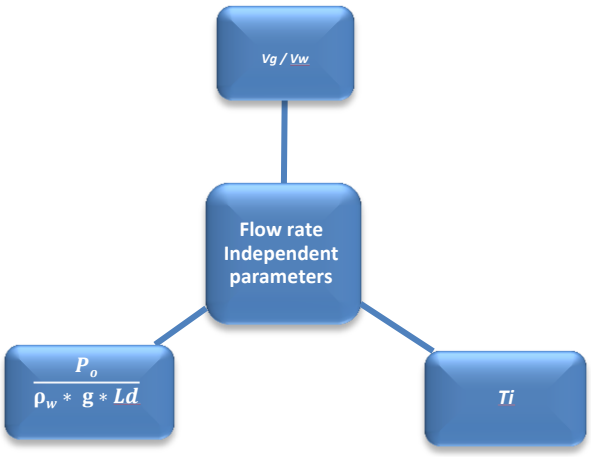

Figure-7 F.P. independent parameters

3 Experimental study

3.1 Experimental Setup

In this section an experimental study is carried out to verify the impact of the controlling parameters such as; Ti and (V_g / V_w) on the performance of the fluidyne pump. An experimental model of the F.P. is designed and constructed. It consists of cast iron tubes with diameter of 0.5 inch (1.125cm). This includes two vertical tubes with 57 cm height (fig.8), which represent the hot and cold tubes. A horizontal connection tube of 20 cm length, which is known as the displacer, has the same diameter. Both the regeneration and the displacer tube have the same diameter.

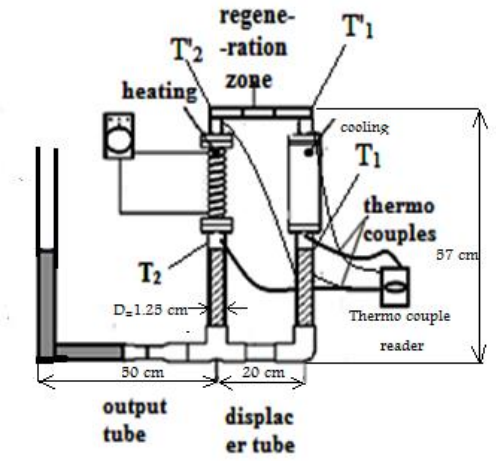

Fig. 8 Schematic of test rig

The regenerator is packed with aluminum wires packing to ensure efficient heat transfer and quick cycling heating and cooling. All the tubes are assembled by cast iron T-joints and 90^0-elbows. The engine is equipped with a plug to control the water level inside the tubes, such that the gas to volume ratio can be changed. As the water is filled to the required gas to liquid ratio, the plug is fixed tightly to ensure there is no air leak. An external heat supply is provided using 100 watt-circular electrical heater surrounding the hot tube. The heating rate is controlled by a variable resistance. The circuit is equipped with a multimeter to measure both the supplied current and voltage to the heater. The heater is thermally insulated by two layers of insulation. These include two half tubular thermal brick sleave of thermal conductivity 0.05 w/m. K· And an external layer of glass wool of thermal conductivity 0.04 w/m. K· This is to ensure that all the heat supplied by the heater is directed to the fluidyne engine. The test rig has the dimensions shown in Table 3

Table (3) basic dimensions of the test rig

Parameter	Dimension (mm)
L_d	200
L_o	500
$D_g=D_d=D_o$	12.5
H_o (for the base case)	54

Four thermocouples T-type are used to measure the temperatures in the hot and the cold air zones as well as the entry and exit of the regenerator. The thermocouples are embedded inside both the cold and hot zones to be able to measure the gas temperature. The installation points for thermocouples are chosen to be high enough above the expected change in the water level due to oscillation. Also, to measure the effectiveness of the regenerator. Two other thermocouples are installed as close as possible to the entry and the exist of the regenerator respectively. Reading of the thermocouples in the cold and hot zones T_1 &T'_1&T'_2 and T_2 respectively are carried out using a thermocouple reader (AX4 – 1A, multi input and multi output) for T-type sensor, 0°C to +400°C, with a total error of ±0.03°C. Where T'_1 and T'_2 are the temperatures of cold and hot inlet and exist of regenerator respectively. When the operation of the engine reaches a steady state and the temperature is fixed for both the cold and hot zones the parameter $T_i = \frac{T2-T1}{T2+T1}$ is calculated, where both T1 and T2 are the average temperatures of both the cold and hot zones respectively.

Stop watch is used measure the onset time. Liquid oscillations are recorded by a camera for one minute, where the number of oscillations is counted and consequently oscillation frequency is calculated. Pumped water flow rate is measured after the "onset" of oscillation. The pumped water quantity is measured using a balance and the corresponding time is measured using a stop watch. These measurements are used to calculate both the engine output work and pump efficiency.

The tested conditions include both loading and un-loading conditions. Figure 9 and 10 show pictures for the test rig. Regarding the conditions covered experimentally, a base case has been defined, as shown in Table 4. To find out the impact of the controlling factors additional four cases for each parameter have been considered for both the gas to liquid ratio and input heat.

Table (4) the conditions covered experimentally

	V_g/V_w	Q_{in} (W)	Number of Runs
Base Case	4	80	1
Effect of V_g/V_w	5,4.5,3.5,3	80	4
Qin/V_g	4	60,70, 90, 100	4
Total Runs			9

The measurements include temperatures of: hot zone, regeneration zone edges and cold zone temperatures, the onset time in minutes, the oscillation frequency and consequently ω (rad/second) and pumped water flow rate (Q^o) in Lit. /min. Based on these measurements' performance parameters are calculated including; FP efficiency and the nondimensional discharge.

Based on a detail error analysis regarding the source of both systematic errors and accidental errors, it has been found that the error in the measured pump efficiency and flow rate is about (+/- 4.2%).

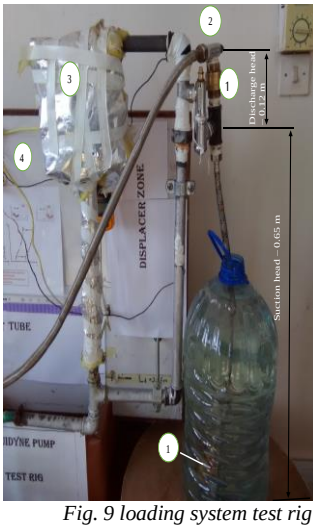

Fig. 9 loading system test rig

1- Non-return valves
2- On/Off valve
3-Circulated heater surrounded by thermal bricks and glass wool
4-Thermo-couples

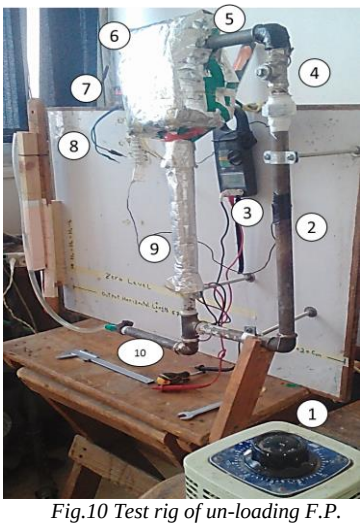

Fig.10 Test rig of un-loading F.P.

1-1 kw Variac
2- cold zone tube - 0.5" diameter
3-hot zone tube – 0.5" diameter
4- clamping amperometer
5-0.5" plug
6- .5" regeneration tube
7- glass wool surrounded the thermal bricks and the circulating heater
8- Thermocouples reader
9- 0.5" output diameter
10- Thermocouples T-type

3.2 Results and Comparison between the computational and experimental results: -

Fertilizer

As shown in Fig. 11, the flow rate increases with the increase in the heat intensity. This conclusion is valid to any pump size providing that the diameters of the tubes are fixed. It is expected that this conclusion will not change as the output tube length (L_o) is changed. Although this change shall affect Q^o as a result of the change in the operation frequency, yet it will affect both the numerator and denominator of the nondimensional quantity. However, there may be a minor impact, as the friction losses increase due to the increase in the frequency.

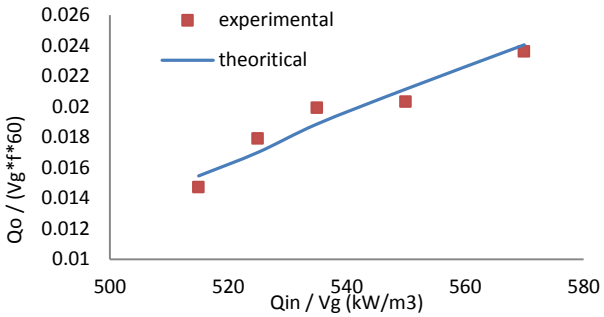

Fig. 11 flow rate for different V_g/V_w, and different input power for base case

On the other hand, the pump discharge increases as V_g/V_w increases, as shown in Fig. 12. Yet the rate of increase is moderated at high values of V_g/V_w. This takes almost a liner relation. As shown from Fig. 12, the experimental results are below the computational one. This may be attributed to the effect of the friction losses, which is not considered in the computational results. On the other hand, the difference between the computational and experimental results is higher at high values of V_g/V_w. This again can be explained as an impact of the friction losses, where at high value of V_g/V_w , the stroke of the liquid piston "R" becomes longer, which increases the friction losses.

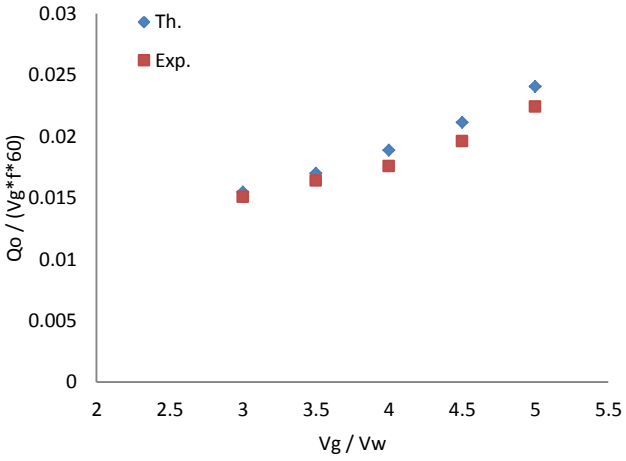

Fig.12 Flow rate at different Vg / Vw)

Regarding the pump efficiency, it can be seen that it improves as the Qin/Vg increases, as shown in Fig. 13. This is mainly attributed to the increase in Ti, as a result of the increase in Qin/Vg, as shown in Fig.14. Where Ti has a strong impact on the pump efficiency, as shown in Fig. 15.

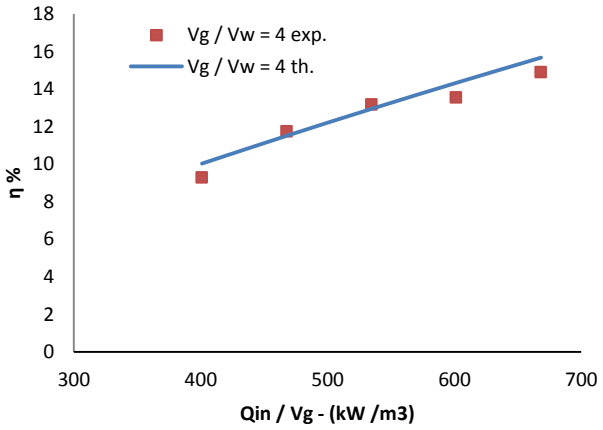

Fig.13 Effect of heat intensity on the efficiency

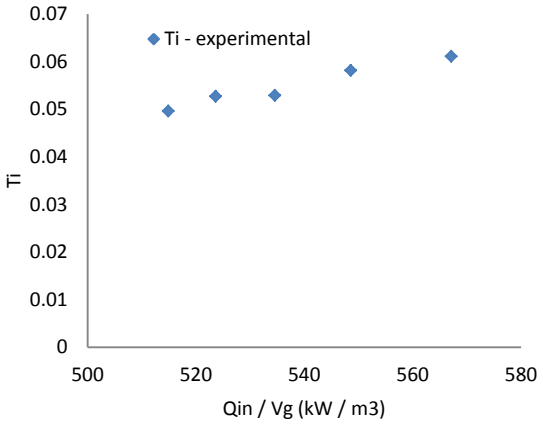

Fig. 14 Effect on input heat intensity on the temperature parameter (Ti)

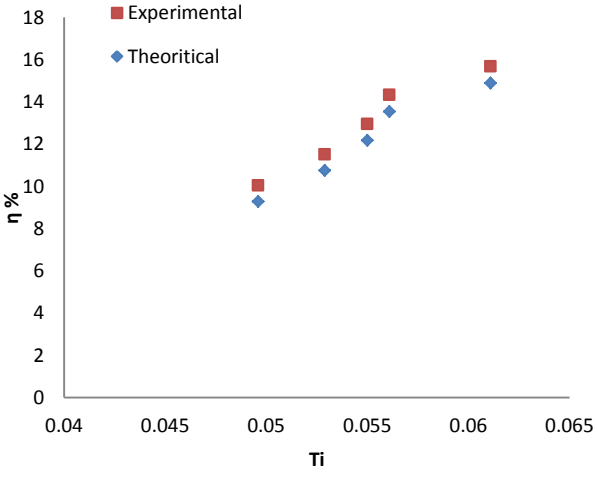

Fig. 15 Effect of temperature parameter (Ti) on the efficiency of the fluidyne pump

Regarding the Onset time of the pump, Fig. 16 shows that, this time become less as the heating intensity become higher. This trend is almost universal for all values of Vg/Vw .

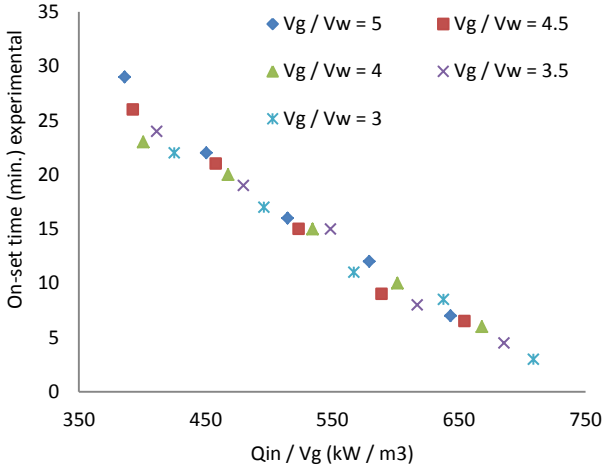

Fig. 16 on-set time at different Q_{in} / Vg

4. Conclusions

The detail analysis of the governing equations of the Fluidyne pump showed that the three controlling parameters; gas to liquid volume ratio, temperature parameter (T_i) and P_o / ρ_w *g*L_d have a controlling impact on the performance indicators of the Fluidyne pump, represented by the pump efficiency and discharge. This has been confirmed through the experimental measurements. It has been found that as V_g/V_l is higher the efficiency of the Fluidyne pump improves. Yet this is limited by the difference (2 P_oT_i /ρ_w*g*L_d) -(V_g / V_w), which should not be negative. Maximum flow rate can be achieved as the difference between 2 P_oT_i /ρ_w*g*L_d) -(V_g / V_w) becomes minimum. Pump efficiency improves due to the increase in both heat intensity and V_g/V_w. Improvement in efficiency due to the increase in heat intensity is mainly attributed to the increase in the temperature parameter T_i, as the heat intensity increases. Furthermore, the onset time becomes less. Both the computational and experimental results are reasonably consistent.

Nomenclature: -

A_d: cross section area of displacer tube[m^2]
A_o: cross section area of output tube[m^2]
A_g: cross section area of gas tube[m^2]
b: velocity dependent load coefficient [N.m/s]
D_d: diameter of displacer tube [m]
D_g diameter of gas tube[m]
D_o: diameter of output tube[m]
g: gravity acceleration[m/s^2]
H_h: heights of output column [m]
H_c: heights of cold column[m]
H_o: heights of output column[m]
H : H= Ho= H_c= H_h, for balancing case
h: total head[m]
L_d: horizontal length of displacer [m]
L_o: total length of output tube [m]
L_w: total length of working liquid tube [m]
L_g: total length of working gas tube [m]
P_o: output tube pressure [pas]
P_a: atmospheric pressure [101k.pas]
Q^o: volumetric flow rate [m^3/s]

R: Amplitude [m]
T_1: temperatures of cold zone [k^o, C^o]
T_2: temperatures of hot zone [k^o, C^o]
V_g: working gas volume [m^3]
V_w: working liquid volume [m^3]
Greek:
γ_w: Kinematic viscosity of working liquid[m^2/s]
ρ_o: density of output liquid[kg/m^3]
ρ_w: density of working liquid[kg/m^3]
ω: radian frequency [rad/sec]
ω_{un}: *unloading radian frequency [rad/sec]*
ω_l:*nloading radian frequency [rad/sec]*
μ_w: absolute viscosity for working liquid [pas. s]
Q_{in}::input power

Subscription:
d_i: working liquid length factor $d_i=\frac{L_d}{2H+L_d}$ *[-]*
T_i: temperature factor $T_i=\frac{T_2-T_1}{T_2+T_1}$*[-]*
Abbreviations:
F.P. : fluidyne pump

References

[1] D.C. Mosby " The fluidyne heat engine", MSc Thesis, Naval Postgraduate School, USA, (1978).
[2] C. W. STAMMERS " The Operation of The Fluidyne Heat Engine at Low Differential Temperatures "Journal of Sound and Vibration 63(4), 507-516. (1979)
[3] C.D. West " Liquid piston Stirling energy " Van Nostrand company – 1983
[4] G. Walker and J. R. Senft - (Lecture Notes in Engineering)- Springer-Verlag Free Piston Stirling Engines Berlin Heidelberg New York Tokyo - 1985
[5] L.F. Goldberg, (A Computer Simulation and Experimental Development of Liquid Piston Stirling Cycle Engines). M.Sc. Dissertation, University of the Witwatersrand, Johannesburg, Mar. 1979
[6] G.T. Reader, and P.D. Lewis, (The Fluidyne - Water in Glass Heat Engine). (1979b). M.N.S., Vol. 5, No.4, pp. 240-245.
[7] G.C Bell, (Solar Powered Liquid Piston Stirling Cycle Irrigation Pump). SAN-1894/1, April 1979
[8] R.B. Pendey, and C. West, (A Laboratory Prototype Fluidyne Water Pump. Paper) No. 819787, Proc. 16th Inter. Soc. Energy Cony. Eng. Conf., Atlanta. Ga., Aug. (1981).
[9] Y.Yoshiyuki - " STUDY ON WATER-TYPE STIRLING ENGINE AND ITS REVERSE CYCLE Division of Heat Transfer " - Department of Energy Sciences, Faculty of Engineering, Lund University - …. 2009
[10] F. KYEI-MANU, A. OBODOAKO " Design and Development of a Liquid Piston Stirling Engine " E90 Senior Design Project Report May 2 2006.
[11] C.D. West "Stirling engines and irrigation pumping" National Technical Information Services, USA 1987.
[12] M. Delgado and D.C.G. Sánchez, (Fı´sica Fundamentaly Experimental, Electro´nica y Sistemas), Universidad de La Laguna, Spain – 2009
[13 D. G. Chadwick " Design of a Cost Effective Solar Powered Water Pump", Utah Water Research Laboratory 1980
[14] C. C. Lloyd " A LOW TEMPERATURE DIFFERENTIAL STIRLING ENGINE FOR POWER GENERATION " University of Canterbury 2009
[15] S. Narayan, A. Gupta, R. Rana " PERFORMANCE ANALYSIS OF LIQUID PISTON FLUIDYNE SYSTEMS "Department of Mechanical Engineering, Indus University, INDIA
[16] J.W. Mason, J.W. Stevens " Characterization of a solar-powered fluidyne test bed " - Sustainable Energy Technologies and Assessments, vol 8. 1-8 2014.
[17] A. D. Minassians " Stirling Engines for Low Temperature Solar Thermal Electric Power Generation", Technical Report No. UCB/EECS-2007-172, Electrical Engineering and Computer Sciences University of California at Berkeley ….. December 2007.